

Stroke

American Stroke
AssociationSM

A Division of American
Heart Association



JOURNAL OF THE AMERICAN HEART ASSOCIATION

Effect of Aging on Elastin Functionality in Human Cerebral Arteries

Edouard Fonck, Georg G. Feigl, Jean Fasel, Daniel Sage, Michael Unser, Daniel A. Rüfenacht and Nikolaos Stergiopoulos

Stroke 2009;40;2552-2556; originally published online May 28, 2009;

DOI: 10.1161/STROKEAHA.108.528091

Stroke is published by the American Heart Association, 7272 Greenville Avenue, Dallas, TX 72514
Copyright © 2009 American Heart Association. All rights reserved. Print ISSN: 0039-2499. Online
ISSN: 1524-4628

The online version of this article, along with updated information and services, is
located on the World Wide Web at:

<http://stroke.ahajournals.org/cgi/content/full/40/7/2552>

Subscriptions: Information about subscribing to Stroke is online at
<http://stroke.ahajournals.org/subscriptions/>

Permissions: Permissions & Rights Desk, Lippincott Williams & Wilkins, a division of Wolters
Kluwer Health, 351 West Camden Street, Baltimore, MD 21202-2436. Phone: 410-528-4050. Fax:
410-528-8550. E-mail:
journalpermissions@lww.com

Reprints: Information about reprints can be found online at
<http://www.lww.com/reprints>

Effect of Aging on Elastin Functionality in Human Cerebral Arteries

Edouard Fonck, PhD; Georg G. Feigl, MD; Jean Fasel, MD; Daniel Sage, PhD; Michael Unser, PhD; Daniel A. Rüfenacht, MD; Nikolaos Stergiopoulos, PhD

Background and Purpose—Aging affects elastin, a key component of the arterial wall integrity and functionality. Elastin degradation in cerebral vessels is associated with cerebrovascular disease. The goal of this study is to assess the biomechanical properties of human cerebral arteries, their composition, and their geometry, with particular focus on the functional alteration of elastin attributable to aging.

Methods—Twelve posterior cranial arteries obtained from human cadavers of 2 different age groups were compared morphologically and tested biomechanically before and after enzymatic degradation of elastin. Light, confocal, and scanning electron microscopy were used to analyze and determine structural differences, potentially attributed to aging.

Results—Aging affects structural morphology and the mechanical properties of intracranial arteries. In contrast to main systemic arteries, intima and media thicken while outer diameter remains relatively constant with age, leading to concentric hypertrophy. The structural morphology of elastin changed from a fiber network oriented primarily in the circumferential direction to a more heterogeneously oriented fiber mesh, especially at the intima. Biomechanically, cerebral arteries stiffen with age and lose compliance in the elastin dominated regime. Enzymatic degradation of elastin led to loss in compliance and stiffening in the young group but did not affect the structural and material properties in the older group, suggesting that elastin, though present in equal quantities in the old group, becomes dysfunctional with aging.

Conclusions—Elastin loses its functionality in cerebral arteries with aging, leading to stiffer less compliant arteries. The area fraction of elastin remained, however, fairly constant. The loss of functionality may thus be attributed to fragmentation and structural reorganization of elastin occurring with age. (*Stroke*. 2009;40:2552-2556.)

Key Words: elastin and aging ■ elasticity and stiffness ■ structural properties ■ cerebral arteries

In contrast to abundant information available on the histopathology and morphology of human cerebral arteries,¹ there is still little known on how changes in wall constituents, as assessed by histology and morphology, are reflected on the biomechanical properties of the wall, such as wall elasticity and compliance. Hence, there is a missing link between histomorphological changes happening with aging and the corresponding effects in biomechanical/functional properties of the cerebral artery wall. To address this issue, the present work focuses on the effects of aging on histomorphometry and biomechanical properties of the cerebral artery wall, with particular emphasis on the functional integrity of elastin.

Methods

Left posterior cerebral arteries (PCAL) were collected from young (42.2 ± 3.8 years old; $n=6$) and old (70.3 ± 12.5 years old; $n=6$) subjects within 12 hours postmortem at the Pathology Department of the Medical University of Graz, Austria. Table A provides demo-

graphic information for each subject. Arteries were treated by enzymatic degradation following the protocol described by Fonck et al.²

Histological Analysis

Arteries were stained with Aldehyde-Fuchsin (AF) and Hematoxyline-Eosine (HE). HE stained vascular smooth muscle (VSM) cell nucleus in blue and the extracellular matrix (ECM) in pink. AF staining revealed elastin (purple), collagen network (green), and VSM cells (brown). Histological images (at $5\times$ magnification not shown) were analyzed to qualitatively assess the relative abundance of the 3 wall constituents.³

Elastin and collagen fibers were visualized in the green and red spectra, respectively, using confocal microscopy. Elastin natural auto-fluorescence was used to assess the degree of its fiber alignment in the circumferential direction. The fiber alignment measurement was carried out with a novel ImageJ plug-in that we developed, named "OrientationJ," to calculate the directional coherency coefficient of the elastin fibers (Supplemental Appendix, available online at <http://stroke.ahajournals.org>). A coherency coefficient close to 1, represented as a slender ellipse, indicates a strongly coherent orientation of the local fibers in the direction of the ellipse long axis.

Received October 5, 2008; accepted February 23, 2009.

From the Laboratory of Hemodynamics and Cardiovascular Technology (E.F., N.S.), Swiss Federal Institute of Technology, Lausanne, Switzerland; the Institute of Anatomy (G.G.F.), Medical University of Graz, Austria; the Division of Anatomy, Department of Morphology (J.F.), CMU Geneva, Switzerland; the Biomedical Imaging Group (D.S., M.U.), Swiss Federal Institute of Technology, Lausanne, Switzerland; and the Neurointerventional Division, Clinical Neuroscience Department (D.A.R.), Geneva University Hospital, Switzerland.

Correspondence to Edouard Fonck, Laboratory of Hemodynamics and Cardiovascular Technology, 1015 Lausanne, Switzerland. E-mail edouard.fonck@a3.epfl.ch

© 2009 American Heart Association, Inc.

Stroke is available at <http://stroke.ahajournals.org>

DOI: 10.1161/STROKEAHA.108.528091

Table. A. Demographic

Subject	Parameters	Young	Old
1	Sex	Female	Male
	Age, y	41	81
	Weight, kg	50	69
	Height, cm	160	175
	Cause of death	Hepatic insufficiency	Renal insufficiency
	Illness	Pulmonary metastasis	Hypertonia
2	Sex	Female	Male
	Age, y	40	63
	Weight, kg	79	77
	Height, cm	173	182
	Cause of death		Myocardial infarct
	Illness	Cerebral haemorrhage pulmonary artery embolism, dilatative cardiomyopathy	Cardiac decompensation
3	Sex	Male	Female
	Age, y	39	52
	Weight, kg	85	60
	Height, cm	180	170
	Cause of death	Pulmonal decompensation, sepsis Mb Wegener	Pulmonal insufficiency
	Illness		Mammary carcinoma
4	Sex	Female	Female
	Age, y	44	66
	Weight, kg	175	70
	Height, cm	70	165
	Cause of death	Cardiac insufficiency	Cardiac arrest, giant ruptured cerebral aneurysm (d=3 cm), cerebral infarct (diencephalic)
	Illness		
5	Sex	Female	Male
	Age, y	50	87
	Weight, kg	60	65
	Height, cm	165	170
	Cause of death	Gastro-intestinal bleeding hepatic cirrhosis	Cardiac decompensation diabetes, aortic stenosis, bladder cancer
	Illness		
6	Sex	Male	Male
	Age, y	49	73
	Weight, kg	90	80
	Height, cm	190	175
	Cause of death	Multiple organ failure	Myocardial infarct
	Illness	Hepatic cirrhosis	Coronary sclerosis

B.

Parameters	Young (n=6)	Old (n=6)	P
Age, y	42.2±3.7	70.3±12.5	<i>P</i> <1E-4
Thickness (mm) at 100 mm Hg	0.17±0.01	0.25±0.02	<i>P</i> <1E-4
Inner Diameter (mm) at 100 mm Hg	2.36±0.05	2.27±0.07	N.S
Thickness/radius ratio at 100 mm Hg	0.15±0.01	0.21±0.03	<i>P</i> <1E-4
Opening angle,°	143.8±15.4	100.9±25.4	<i>P</i> <0.01

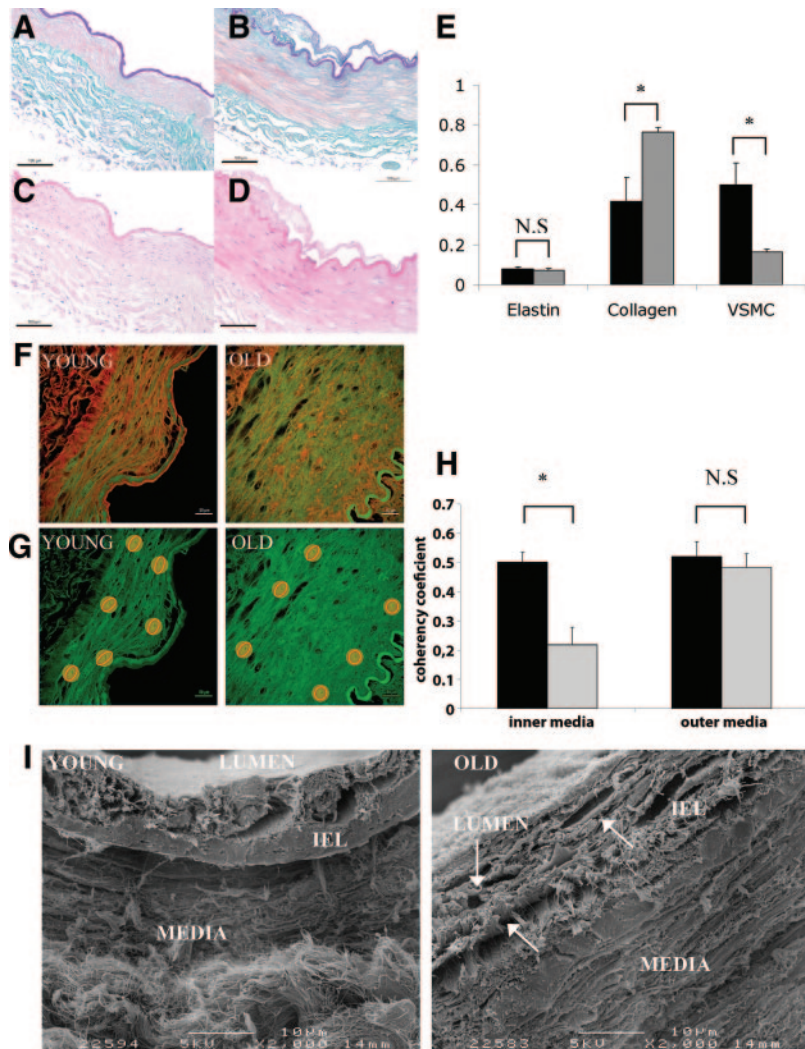


Figure 1. Cross-sections of posterior cerebral arteries of young (A and C) and old (B and D) specimens stained with Aldehyde-Fuchsin (A and B), illustrating elastin (purple), collagen (green), and VSM cells (brown) and Hematoxyline-Eosine (C and D) illustrating the ECM (pink) and VSM cell nucleus (blue). Scale bar, A through D: 100 μ m. E, Relative mean area fraction and SD of elastin, collagen, and VSM cells in both young (black) and old groups (gray). * P <0.05; NS indicates nonsignificant. F, Confocal microscopy images (63 \times) differentiating elastin (green) from collagen (red) in young and old specimens. G shows only the elastin matrix from which coherency coefficients were calculated in the inner and outer media. Scale bar, F and G: 50 μ m. H, Mean values and SD of coherency coefficients of young (black) and old (gray) specimens in the inner and outer media. * P <0.05; NS indicates nonsignificant. I, Electron microscopy images illustrating the fragmentation of the IEL in an old specimen compared to young specimen at 2000 \times magnification. Arrows show the fragmented elastin fibers in the old specimen.

A coherency coefficient close to zero, represented geometrically as a circle, denotes no preferential orientation of the fibers. The fine structure of the arterial wall was revealed by scanning electron microscopy (SEM).

Biomechanical Analysis

External diameter-pressure curves were combined with the zero load state geometric data (opening angle, internal and external radius) and processed to derive internal diameter-pressure curves, distensibility, and incremental elastic modulus.² We refer the reader to our previous article² for further information on the methods used.

Results

Histology

Young arteries (Figure 1A and 1C) show a thinner media composed of a higher number of VSM cells, compared to old arteries (Figure 1B and 1D). The semiquantitative assessment of relative mean area fraction of the components is displayed in Figure 1E. The increase in wall media area in old arteries is accompanied by a noticeable increase in the fractional area of collagen and a significant decrease in VSM cells. In contrast, the fractional area of elastin did not vary significantly (P >0.05). Figure 1F shows structural differences of the elastin fibers, which are organized in layers/lamellae in

the young arteries which seem to be randomly distributed in the older arteries. Elastin fibers of aged arteries appear as a set of separate thinner elastic fibers compared to the thick elastic lamina seen in young arteries. Figure 1G displays confocal images of both groups in the green channel. It shows also the coherence in elastin fiber orientation, as shown geometrically by ellipses (red) in the regions of interest (yellow). Figure 1H displays the average values of coherency coefficients and their standard deviations (SD) of both groups, for the inner and outer media regions. The directional analysis showed disperse fiber orientation in the inner media (coherency coefficient of 0.22 ± 0.06) in the old group as opposed to a coherent circumferential fiber orientation seen in the inner media (coherency coefficient of 0.50 ± 0.03) in the young group. The loss in coherent directionality of elastin fibers in the old group is much more pronounced in the inner media (0.22 ± 0.06) rather than the outer media (0.48 ± 0.05).

Figure 1I displays the SEM micrographs of the fine structure of the young and old specimens at 2000 \times magnification. The internal elastic lamina (IEL) is present in both young and old specimens but is structurally different. In young subjects it appears as a thick, continuous, and compact

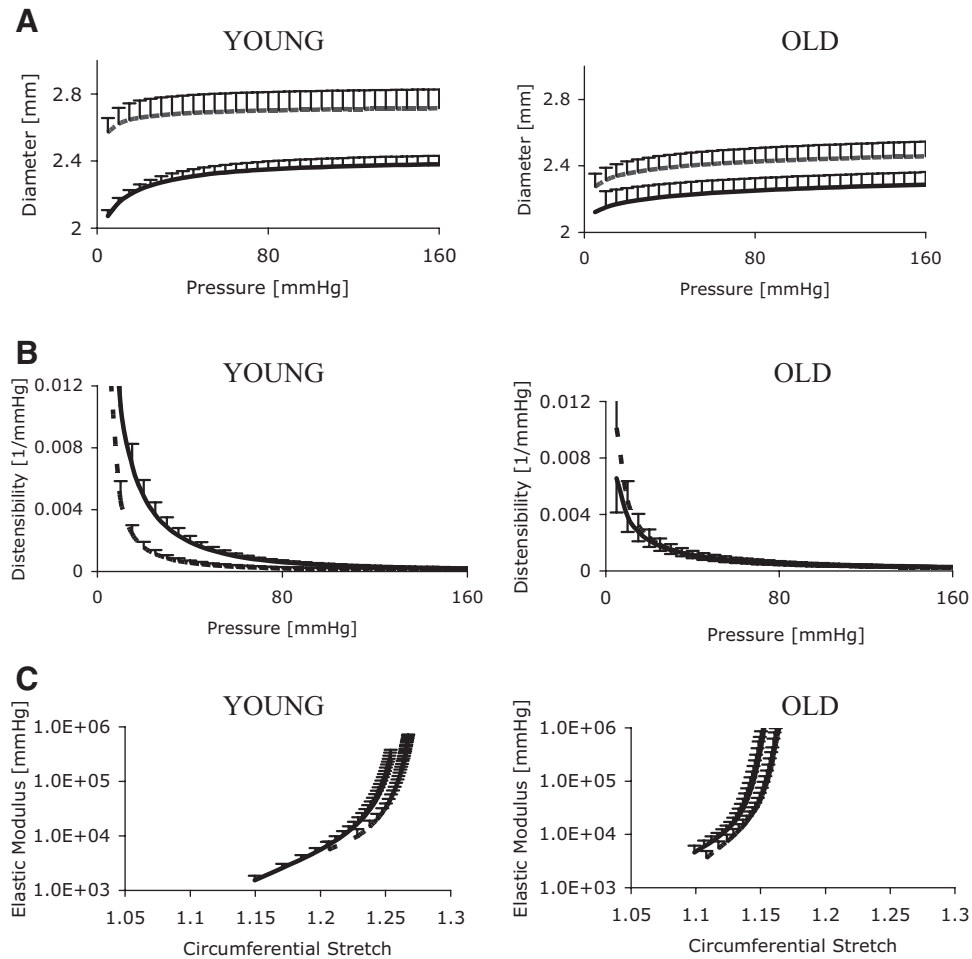


Figure 2. A, Pressure-diameter curves of control (n=6; solid lines) and elastase treated (n=6; dashed lines) for both young and old groups. B, Pressure-distensibility curves of control (n=6; solid lines) and elastase treated (n=6; dashed lines) for both young and old groups. C, Incremental elastic modulus vs. midwall circumferential stretch ratios of control (n=6; solid lines) and elastase treated (n=6; dashed lines) for both young and old groups.

layer. In contrast, in the old subjects, IEL presents a stratified structure composed of multiple thinner layers of elastin. In addition, these layers appear to be fragmented and discontinuous (as pointed out by the white arrows) in the circumferential direction.

Biomechanical Analysis

Pressure-diameter (p-d) curves are shown in Figure 2A before (solid lines) and after elastase treatment (dashed lines). The mean inner diameter of the young group (n=6) displayed higher values over the physiological pressure range in comparison to the mean inner diameter of arteries from old subjects (n=6) before and after elastin fragmentation, suggesting an inward remodeling of the wall in the aged group. Elastase treatment led to a higher diameter increase at low pressures in the young group as compared to the old group, suggesting that higher levels of compressive prestresses were released on destruction of elastin in the young group. This is not the case in the old group, where p-d curves of both control and treated arteries exhibit similar shapes and slopes, suggesting that destruction of elastin did not alter the inherent structural properties of the arterial wall. This is reflected into the old group distensibility-pressure curves (Figure 2B),

which are remarkably similar before (solid lines) and after enzymatic treatment (dashed lines). In contrast, digestion of the elastin in the young group led to a significant decrease in distensibility.

Incremental elastic modulus (E_{inc}) is shown in Figure 2C for both groups, before and after elastase treatment. At comparable degrees of circumferential stretch (λ_z), aging increased dramatically the stiffness of the arterial wall. Young arteries present “ductile material” characteristics in the low circumferential stretch regime ($\lambda_z < 1.22$), indicative of a functional load-bearing elastin. In contrast, old arteries are already stiff at low circumferential stretch ratios and become abruptly stiffer on further stretching. This indicates lack of functional elastin and early engagement of collagen, even at low levels of hoop stretch. Fragmenting the elastin of the young group shifts the E_{inc} - λ_z curve to the right and yields a collagen-dominated curve, similar in shape to those of old control arteries. Apart from a slight shift to the right, elastin destruction does not alter the E_{inc} - λ_z curve in the old group, which indicates that elastin, although histologically present, contributes less to the material properties of the wall. This is also reflected in the diminution of the opening angle reported in Table B for the elder arteries as compared to the young group.

Discussion

We analyzed the morphological and geometric changes of human intracranial arteries, assessed their mechanical properties, and characterized the effects of further elastin degradation in 2 distinct groups of age. Even though elastin fractional area remained constant in both age groups, there appears to be substantial loss of elastin functionality with age, mainly attributable to structural changes in the elastin fibers organization.

Vessel Histology and Morphology

There are noticeable changes in morphology of the wall during aging. Old arteries showed an inward thickening of the intima-media layer responsible for approximately 8% reduction of the lumen area. Histomorphological findings revealed no significant differences in the relative fractional area of elastin between the 2 age groups. Similar findings for the thoracic aorta were reported by Spina et al,⁴ although others have reported loss of absolute elastin content in other human arteries.^{5,6} These observations do not exclude differences in elastin functionality with age, impacting on the mechanical properties of the wall. Confocal microscopy revealed remarkable differences in elastin macro-structure in aged arteries as compared to young. Indeed, elastin of the young group is structurally organized circumferentially whereas elastin of the old group is distributed heterogeneously throughout the wall and lacks coherent orientation, primarily in the inner media (Figure 1G). The principal difference in the micro-structure between young and old subjects lies in the structural characteristics of the IEL. As seen clearly in Figure 1I, the IEL of young subjects is thick and continuous, and being the stress bearing structure at lower pressures, may contribute to the compliance of the vessel.² In contrast, IEL in old subjects is composed of multiple fragmented layers, thus functionally unable to bear load and contribute to compliance.

Biomechanical Changes

Aging impacts the distensibility and elastic modulus of the arterial wall. Wall stiffening is almost entirely attributed to the structural changes in the elastin network, as discussed above. Destruction of the elastin of young PCAL significantly altered the biomechanical properties of the arterial wall, as seen on the distensibility and on the elastic modulus shown in Figure 2B and 2C. In contrast, degradation of elastin in aged PCAL did not markedly modify their biomechanical properties. These results, in conjunction with the relatively constant fractional area of elastin in the 2 age groups, led us to the main conclusion that elastin is not reduced but becomes dysfunctional with aging. Structural integrity and integration are thus important factors.⁷ Similar conclusions have been drawn earlier on the role of structural parameters of collagen

(rate of collagen fiber engagement when exposed to strain) on the compliance of the aging human aorta.⁸

Limitations

Image analysis does not permit accurate measurements of wall component content. Enzymatic treatments could imply collateral structural changes of collagen fibers and may not be effective and complete to the same degree in all samples.

Conclusions

We conclude that the loss of distensibility with aging is not related to loss of elastin fibers but to fragmentation and change in structural organization of elastin fibers. Nonfunctional elastin and increased stiffness affects a number of biological functions on the arterial wall and may be implicated in various forms of cerebrovascular disease.

Acknowledgments

We acknowledge Dr Wohlwend, Heimo Ulz, Dr Sylvain Roy, and Prof Kleinert and his team for their valuable collaboration.

Sources of Funding

This work was supported by the Swiss National Science Foundation, Grant 510691.

Disclosures

None.

References

1. Stehens WE. Arterial structure at branches and bifurcations with reference to physiological and pathological processes, including aneurysm formation. In: Press P, ed. *Structure and Function of the Circulation*. 1981:667–693.
2. Fonck E, Prod'homme G, Roy S, Augsburg L, Rufenacht DA, Stergiopoulos N. Effect of elastin degradation on carotid wall mechanics as assessed by a constituent-based biomechanical model. *Am J Physiol Heart Circ Physiol*. 2007;292:H2754–H2763.
3. Zulliger M, Fridez P, Hayashi K, Stergiopoulos N. A strain energy function for arteries accounting for wall composition and structure. *J Biomech*. 2004;37:989–1000.
4. Spina M, Garbisa S, Hinnie J, Hunter JC, Serafini-Fracassini A. Age-related changes in composition and mechanical properties of the tunica media of the upper thoracic human aorta. *Arteriosclerosis*. 1983;3:64–76.
5. Avolio AP, Deng FQ, Li WQ, Luo YF, Huang ZD, Xing LF, O'Rourke MF. Effects of aging on arterial distensibility in populations with high and low prevalence of hypertension: Comparison between urban and rural communities in china. *Circulation*. 1985;71:202–210.
6. Virmani R, Avolio AP, Mergner WJ, Robinowitz M, Herderick EE, Cornhill JF, Guo SY, Liu TH, Ou DY, O'Rourke M. Effect of aging on aortic morphology in populations with high and low prevalence of hypertension and atherosclerosis. Comparison between occidental and chinese communities. *Am J Pathol*. 1991;139:1119–1129.
7. Laurent S, Boutouyrie P, Lacolley P. Structural and genetic bases of arterial stiffness. *Hypertension*. 2005;45:1050–1055.
8. Zulliger MA, Stergiopoulos N. Structural strain energy function applied to the ageing of the human aorta. *J Biomech*. 2007;40:3061–3069.